Mining, Metallurgy & Exploration (2019) 36:765–772
https://doi.org/10.1007/s42461-019-0064-8

Towards a Field-Portable Real-Time Organic and Elemental Carbon Monitor

D. A. Parks[1] · K. V. Raj[1] · C. A. Berry[1] · A. T. Weakley[2] · P. R. Griffiths[3] · A. L. Miller[1]

Received: 11 December 2018 / Accepted: 20 March 2019 / Published online: 22 April 2019

Abstract
Diesel particulate matter (DPM) has been classified as a carcinogen to humans by the International Agency for Research on Cancer. As a result of its potential carcinogenic nature, DPM exposure is regulated by the Mine Safety and Health Administration. Currently, diesel emissions in the workplace are monitored by collecting the aerosol onto filters, which are then sent to a laboratory for thermal-optical analysis using the NIOSH method 5040. This process can take days or even weeks, and workers can potentially be exposed to excessive levels of DPM before the problem is identified. Moreover, the delay involved in getting the loaded filter to the lab inevitably means the loss of some of the more volatile organic carbon. To remedy this delay, researchers from the National Institute for Occupational Safety and Health are seeking to develop a field-portable, real-time method for measuring elemental and organic carbons in DPM aerosols. In the current study, the use of mid-infrared spectrometry was investigated. It is believed that mid-infrared spectroscopy is more suitable for use in a real-time field-portable device than thermo-optical analysis methods. This article presents a method for measuring organic carbon (OC) and elemental carbon (EC) in DPM for a broad range of OC/EC ratios. The method has been successfully applied to laboratory-generated and mine samples.

Keywords Diesel particulate matter · Organic carbon · Elemental carbon · Real-time monitor

1 Introduction

Health studies have shown a correlation between workplace exposure to diesel exhaust and increased risk of lung cancer [1–7]. Due to the preponderance of evidence indicating the carcinogenic effect of diesel particulate matter (DPM), a permissible exposure limit (PEL) of 160 μg/m^3 (time weighted average over 8 h) total carbon (TC) was instituted for U.S. mines by the Mine Safety and Health Administration (MSHA) in 2008. Although typical levels in mines have been decreasing since the implementation of the PEL and a corresponding increase in monitoring, DPM overexposures continue to occur (Fig. 1).

Previous efforts have sought to develop a real-time DPM monitor [8–10], which has resulted in several commercially available instruments that measure light extinction in the optical regime which, under ideal circumstances, can be attributed to elemental carbon (EC). To obtain total carbon (TC) from EC, one must assume that organic carbon (OC) is proportional to EC with a known constant of proportionality. OC/EC ratios have been shown to be roughly constant for aerosols derived from different sources [11]. In principle, this implies that TC may be estimated, given knowledge of EC for a particular source, to the first approximation. However, it is important to pay close attention to OC/EC ratios as there is evidence they may deviate due to the use of diesel exhaust after-treatment technologies and the increasingly widespread use of biodiesel [12]. With this in mind, it is desirable to develop a method which makes no assumptions about the proportionality of OC to EC, but rather measures a feature which correlates to both EC and OC individually.

There is also currently some debate [13] over whether the mass concentration of particulate carbon is the appropriate metric for health effects given the evolution of DPM in recent and coming years. Although this is not addressed in this paper, it is worth noting that mid-infrared spectrometry has the capability to chemically speciate [14], which may prove useful for future metrics.

✉ D. A. Parks
dparks@cdc.gov

[1] CDC NIOSH, Spokane, WA, USA

[2] University of California Davis, Davis, CA, USA

[3] Griffiths Consulting LLC, Ogden, UT, USA

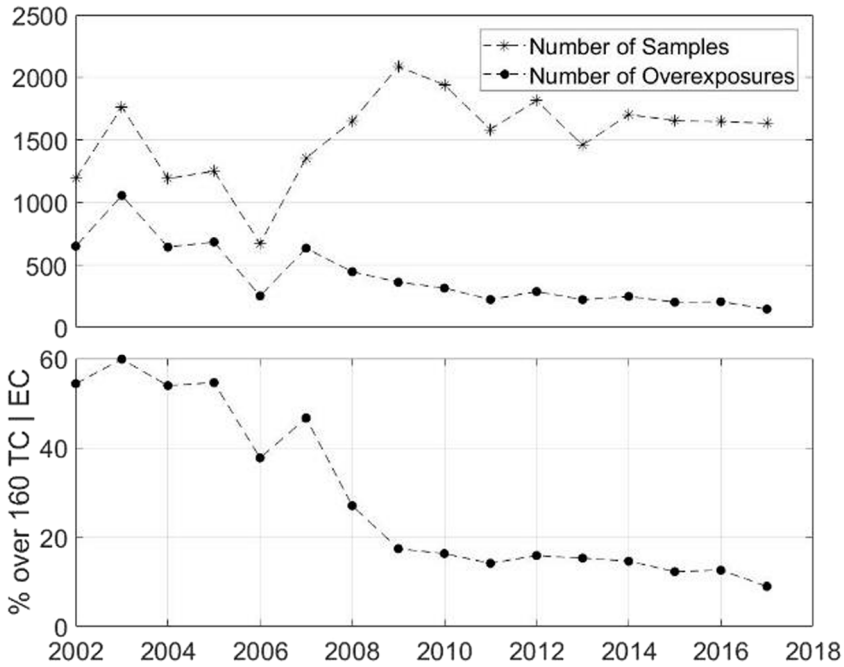

Fig. 1 The number of DPM compliance samples taken by MSHA per year (upper) and the percentage of those samples with TC > 160 μg/m^3 (lower)

In this study, transflectance infrared spectroscopy is utilized to quantify OC and EC as defined by the 5040 method. Here, the quantification is in terms of mass of carbon atoms with no attempt to quantify the true nature or molecular weight of the molecules in either category. It should be noted that there have been numerous other successful quantifications of carbonaceous aerosols by way of FT-IR [14–19]. However, the data presented here are unique in that they represent the first FT-IR prediction of OC and EC as defined by the NIOSH 5040 method. Further, in this study, collocated samples were not needed, rather the same filter on which the 5040 analysis was performed was analyzed directly by way of FT-IR. In this way, artifacts such as loss of semi-volatile organic carbon are avoided. It should also be noted that in [14–19], the scope was significantly broader than that herein in the sense that this study dealt with samples likely containing fewer confounders given samples were taken within mines or directly from laboratory-generated DPM using 0.8 μm cut point as opposed to the 2.5 μm cut point used in the listed works. The MSHA monitoring method requires 0.8 μm; thus, it was used here as well.

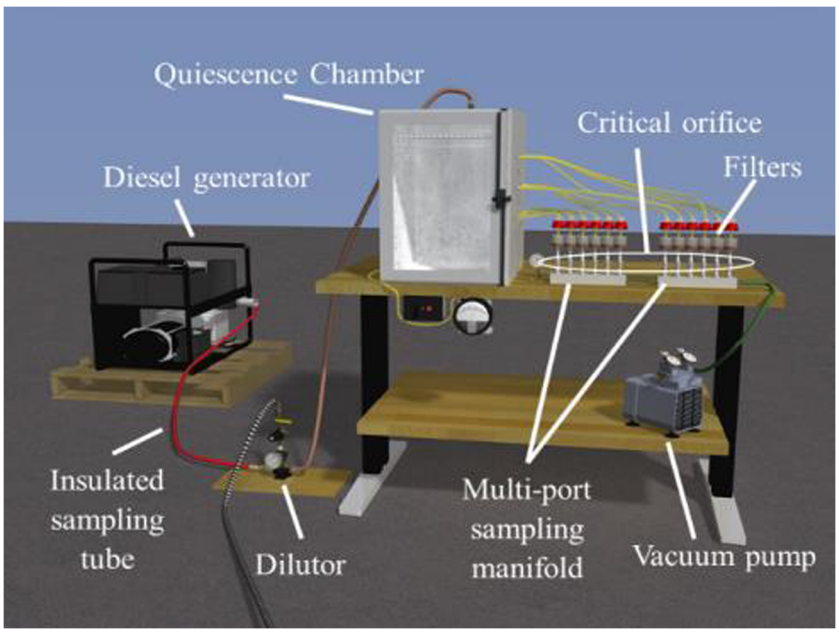

Fig. 2 An illustration of the lab sampling arrangement, with a diesel generator and load bank to represent an operating (loaded) engine

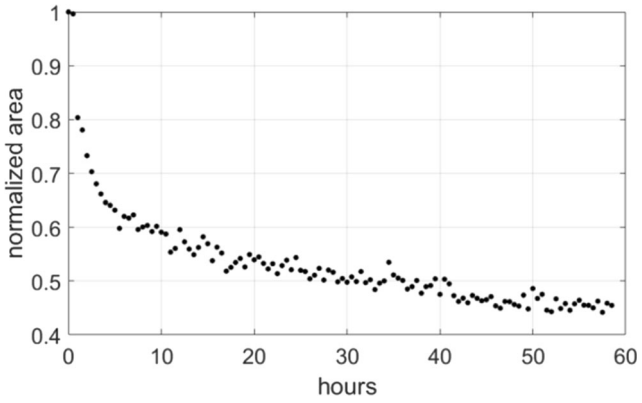

Fig. 3 Loss of volatile OC from a fresh sample measured by integrating the aliphatic C–H stretching bands (2860–2870 cm^{-1})

2 Research Method

2.1 DPM Sampling

To simulate the evolving nature of DPM, specifically the potentially more diverse array of OC/EC ratios [20], several different sampling methods/sources were used in this study. Some of the data used for this proof-of-concept study were generated using a lab-based system, specifically designed for collecting tailpipe samples from a variety of diesel engines. The system consisted of an insulated sampling tube, a dilutor, a quiescence chamber, and a multi-port sampling manifold (Fig. 2). The collection time ranged from 1 to 8 h. The sampling tube was insulated and fitted with a heating tape to prevent premature condensation of volatile DPM aerosols.

The hot stream of raw exhaust was drawn through the insulated sampling tube via the suction provided by the ejector-style dilutor, where it was immediately diluted with cool, dry air. The dilutor was configured to provide approximately a 10:1 dilution ratio, and the secondary airflow exiting the dilutor was directed under slight pressure into a quiescence chamber, where pressure was regulated to ~ 5 mm H_2O above atmospheric pressure by a separate fan and louver control that jettisoned some pressurized air to the ambient atmosphere. The quiescence chamber was fitted with a 12-port manifold, with each port having a 1.7 L/min critical orifice as shown in Fig. 2. The vacuum supplied to the manifold was maintained at > 40 cm Hg to ensure critical flow through the orifices, using a vacuum pump. Standard 37-mm quartz fiber filters in SKC cassettes (with 0.8-μm impactors) were used to collect the DPM. We note that even though Teflon filters are commonly used by the atmospheric chemistry community, we used quartz filters both because the Sunset Laboratory instrument used to provide primary OC and EC values requires (thermally stable) quartz filters and because these filters are specified by MSHA in the regulatory method regarding quantification of worker exposure to DPM.

In addition to the lab-generated samples, 60 samples were obtained from within two different operating mines. The mine samples were obtained using a variety of 1.7 L/min pumps with 0.8-μm impactors and 37-mm SKC quartz fiber filters (as described in the MSHA regulatory method). These samples were obtained by hanging the pumps on the rib and on diesel-powered load, haul dump machines. An effort was made to avoid the roof bolter in order to reduce the influence of oil mist.

The FT-IR and 5040 analyses were done in quick succession so as to minimize loss of volatile OC between the two analysis methods. Additionally, the samples were aged for at least 1 day in a further effort to minimize loss of volatile OC between the two measurements. The aging and quick succession requirements were motivated by the realization that loss of freshly collected volatile OC over relatively short periods of time (even minutes) can be significant as shown in Fig. 3.

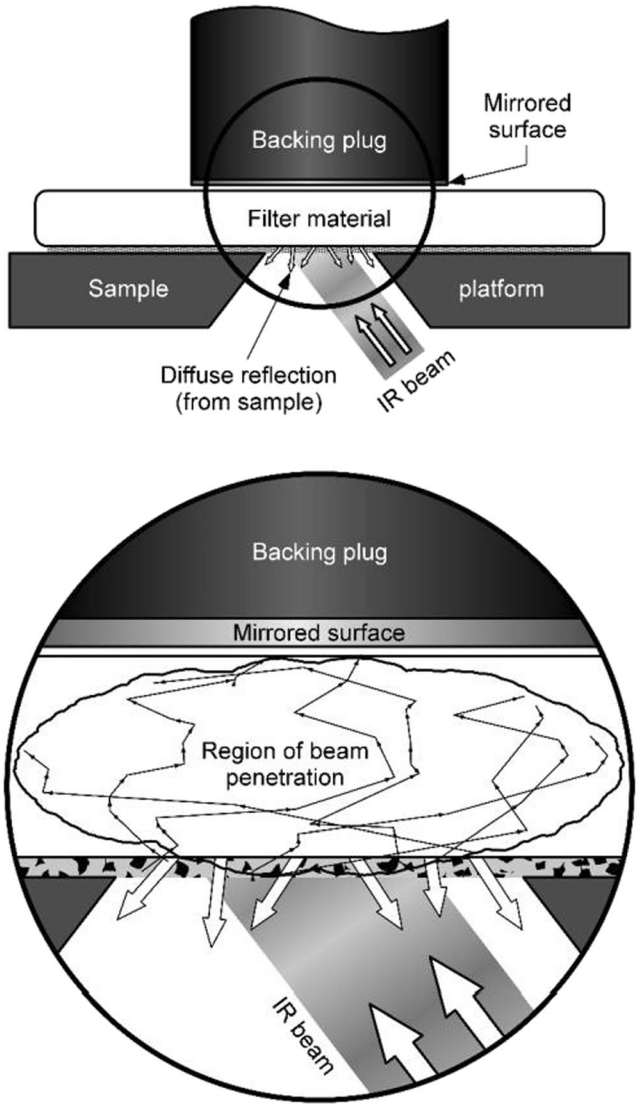

Fig. 4 Artist sketch (not to scale), showing relative geometry of sample placement and beam interaction with the sample

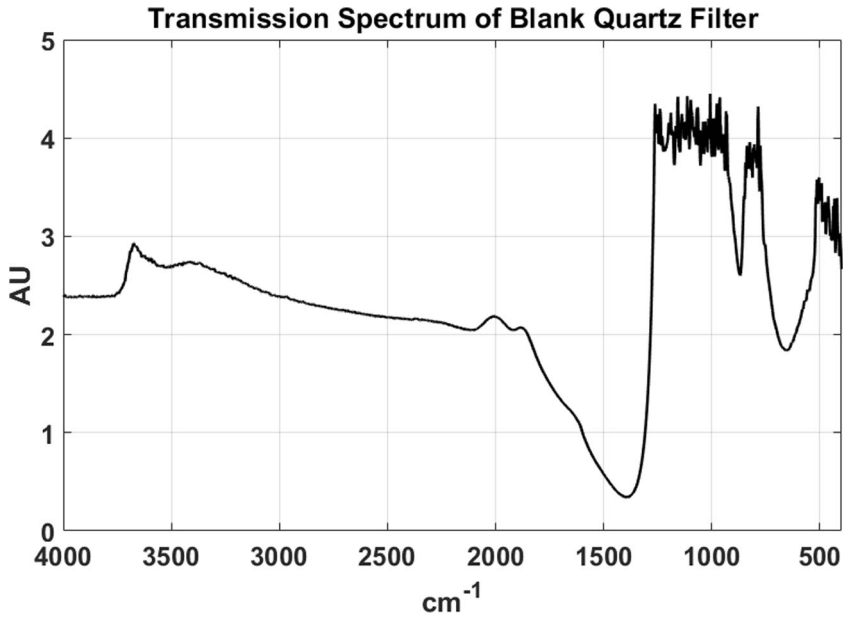

Fig. 5 Transmission mode spectrum of a clean quartz fiber filter showing near-opacity below 1265 cm^{-1}. Note here absorbance is defined as (−log10(*T*)) where *T* is the fraction of light transmitted through the filter

While this issue will be addressed further in our upcoming research, it does imply that the TC value determined when the filter is kept for several days before measurement by an external laboratory is probably less than the actual value in the mine due to evaporation of the OC component.

2.2 Reference Measurement of Organic and Elemental Carbons

The aim of this research is to replicate the NIOSH method 5040 for measuring OC and EC, and to do so by measuring the mid-infrared spectrum and showing correlations to OC and EC. In order to calibrate the infrared data, a Sunset Laboratory Inc. Organic Carbon/Elemental Carbon (OCEC) Laboratory Instrument Model 5L was utilized to measure organic and elemental carbons according to the NIOSH method 5040. A description of this method can be found in [3, 21].

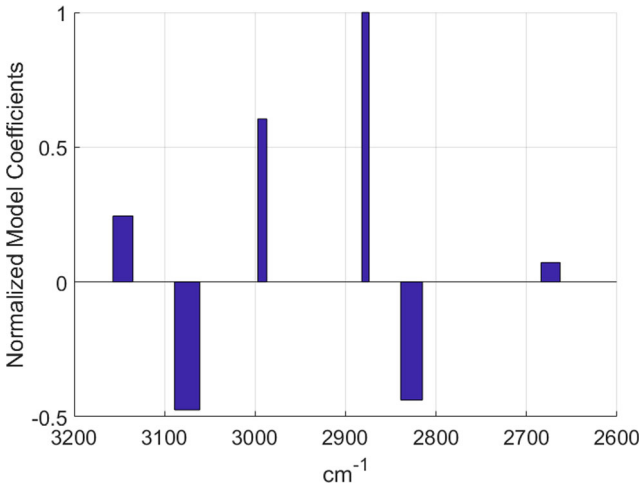

Fig. 6 Normalized model coefficients

2.3 Infrared Spectrometry

The mid-infrared spectrum of each DPM-loaded quartz fiber filter was measured immediately prior to placing it into the Sunset instrument for analysis. The spectra were measured using a Bruker Alpha Fourier transform infrared (FT-IR) spectrometer equipped with a diffuse reflection (DR) accessory that incorporated a gold mirror backing. In the DR module, the infrared beam passes through the thin film of DPM and then enters the quartz fiber filter where it is scattered in all directions. The majority of the forward-scattered radiation is absorbed by the quartz while much of the back-scattered radiation passes again through the DPM, leaves the sample, and is measured by the spectrometer's deuterated triglycine sulfate detector (Fig. 4). The back-scattered light which reaches the detector has therefore passed through the DPM layer twice so that the absorbance of the DPM layer is potentially nearly twice as high as it would have been in a transmission mode measurement. Furthermore, had the spectrum of the filter been measured in the transmission mode, the beam would have been severely attenuated by scattering and absorption below 2000 cm^{-1} and by scattering alone above 2000 cm^{-1} as can be seen in Fig. 5. Scattering reduces the transmittance of the filter above 2000 cm^{-1} to less than 1%. Conversely, the low absorption and the strong scattering of the quartz fiber between 2000 and 4000 cm^{-1} make this region ideally suited for rapid

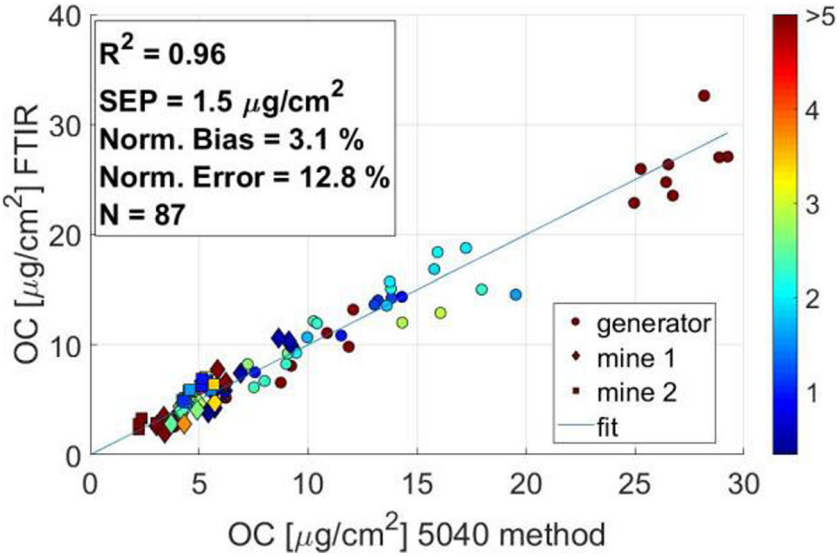

Fig. 7 Correlation between OC and the multiple regression peaks. The color map represents the OC to EC ratio

measurements of the DR spectrum. It can be seen that, even in those spectral regions where the absorption is low (wavenumber $\tilde{\nu} > 2000$ cm^{-1}), the scattering is so large that the absorbance ($-\log_{10}T$) is greater than 2 ($0.001 < T < 0.01$). It is interesting to speculate how deeply the infrared beam penetrates into the quartz filter. Even though the absorption of silica is very weak between 2000 and 4000 cm^{-1}, scattering reduces the intensity of radiation that penetrates more than about 100 μm into the filter to the point that it contributes minimally to the signal measured at the detector. Thus, most of the signal being measured derives from near the upper surface of the filter which is, of course, where most of the DPM that has been collected resides. A spectrum measured by passing the infrared beam through a thin film on the surface of either a metal or a diffusely reflecting substrate such as a ceramic disk is commonly known as a transflection spectrum [16].

In regions of strong quartz absorption ($400 < \tilde{\nu} < 2000$ cm^{-1}), quantification of the thin layer of DPM is not possible by simply converting to $-\log_{10}R(\tilde{\nu})$, where R is the reflectance. Bands in this region appear as maxima in the reflectance spectrum (reststrahlen bands). Thus, below 2000 cm^{-1}, the only rays that return to the detector must be reflected from the front surface of the filter, making quantification extremely difficult. In regions of very strong absorption (e.g., 1100–1000 cm^{-1}), the absorbance is greater than 4 ($T < 0.0001$) so that the signal at the detector is very low and the spectrum is very noisy. In spectral regions where quartz has low absorption ($2000 < \tilde{\nu} < 4000$ cm^{-1}), the reflection mode is diffuse, or volume, reflection, and absorption bands due to either the quartz filter or the DPM on its surface are manifested as minima in the reflectance spectrum. In this spectral region, quantification of the DPM can be achieved by converting the transflectance at wavenumber $\tilde{\nu}$, $R(\tilde{\nu})$, into the pseudo-absorbance $-\log_{10}R(\tilde{\nu})$. This was the method used in this study.

Table 1 Model areas and coefficients

i	Lower limit (cm^{-1})	Upper limit (cm^{-1})	b_i
0	Intercept		5.603324
1	2663	2684	15.48793
2	2815	2839	− 93.8184
3	2987	2997	129.5491
4	3135	3157	52.53998
5	2874	2882	214.1006
6	3061	3089	− 101.635

2.4 Processing of Infrared Spectra for Determining Organic Carbon

It was observed previously [22] that the aliphatic C–H stretching bands were a good candidate for quantification of organic carbon. In an effort to improve the model, a Monte Carlo algorithm was used to find additional areas which correlated well with the OC as measured by way of the method 5040. The Monte Carlo algorithm proceeded as follows:

1. Reduce the spectrum to the aliphatic region while allowing some padding to allow for removal of baseline effects in the region 2500 to 3200 cm^{-1}
2. Choose an upper limit on the width of integration, in this case 50 cm^{-1}
3. Use a random number generator to select 10 areas no wider than 50 cm^{-1} and no narrower than the 2 cm^{-1}

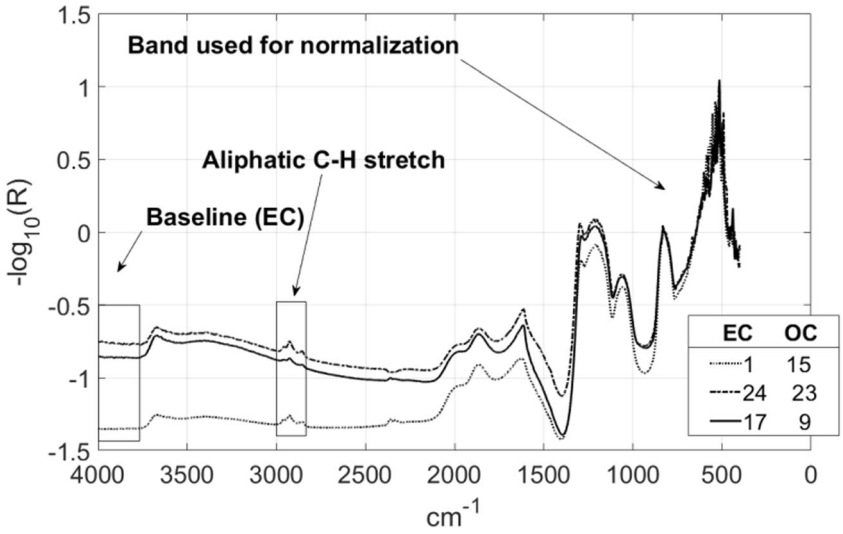

Fig. 8 Transflection spectra normalized to the 822 cm^{-1} peak. Note that OC and EC are in μg/cm^2

4. Utilize ordinary least squares method to find the optimum weighting coefficients for these 10 randomly selected areas in terms of correlation with the OC as measured by the method 5040
5. Remove those areas for which the p value is > 0.05 as they are considered in this case to not significantly improve the model
6. Calculate R^2 and save as the new "fitness" parameter if it is greater than that of all previous iterations, and save the model, replacing the previous best fitting model
7. Repeat

When this process is repeated 100 times, the following areas (Fig. 6) selected for the linear regression model, notice only 6 of 10 areas where retained as the others had a p value > 0.05. In this case, background subtraction was performed on the FT-IR instrument on a regular basis. Since the areas integrated had no significant filter-related confounders, a reference filter was not needed and a simple linear baseline subtraction was found to be sufficient.

The resulting model correlates quite well with the 5040 OC, having r^2 = 0.96 for the diverse range of OC/EC ratio for samples collected in mines or in the laboratories (Fig. 7). Therefore, one calibration may be used to measure OC over a large range of OC/EC ratios. Note the color-bar in Fig. 7 represents the ratio of OC to EC. The range of filter loadings investigated is similar to that which can be expected in a mine environment for an end of shift monitor. However, it should be noted that

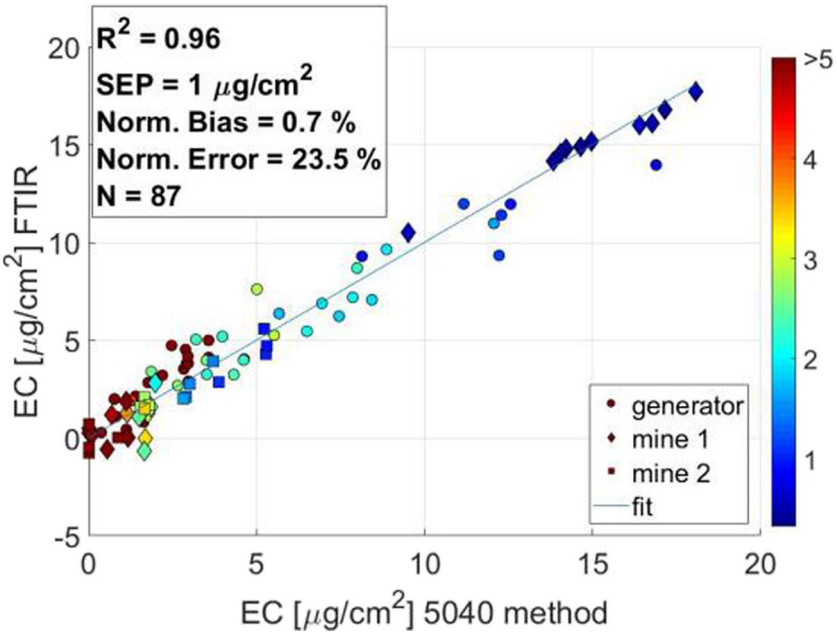

Fig. 9 Correlation between the height of the baseline, after normalization, and the 5040 EC values. The color map represents the OC/EC ratio

the 5040 method is not recommended for use on samples with > 20 μg/cm^2 [21].

The model used here (as found by way of Monte Carlo and ordinary least squares) is of the form

$$OC = b_0 + \sum_{i=1}^{6} b_i A_i$$

where b_i is the coefficient (shown normalized in Fig. 6) and A_i is the corresponding area of integration; the values are provided in Table 1.

2.5 Processing of Infrared Spectra for Determining Elemental Carbon

The particle size of DPM is typically so small (~ 100 nm) and the layer of DPM so thin (< 2 μm) that the deposited DPM contributes minimally to the scattering, most of which arises from the quartz fiber filter. Because the morphology of these filters varies slightly from sample to sample, their scattering coefficient, and hence the baseline of the transflectance spectrum, will also vary. Thus, the spectrum must be normalized prior to quantifying the OC and EC content. With this normalization, Beer's law is now applicable.

It is not expected that either aliphatic or aromatic C–H stretching bands would predict elemental carbon as EC is believed to be composed of graphitic material with little or no hydrogen content. On the other hand, aromatic ring structures found in graphitic carbon and polycyclic aromatic hydrocarbons (PAHs) give rise to a strong, broad electronic absorption band, which is strongest in the visible or ultraviolet region and decays with increasing wavelength [23]. In order to test this theory, the transflection spectra of quartz fiber filters were normalized to the silica peak at 822 cm^{-1} where neither OC nor EC would be expected to have strong vibrational absorption bands, as illustrated in Fig. 8. Normalization was effected by subtracting the value of $-\log_{10}R(\tilde{\nu})$ at 822 cm^{-1} from each point in the spectrum.

When this normalization is performed, it is found that the long-wavelength tail of the broad electronic absorption band of deposited PAH and graphitic material increases the value of the apparent baseline between 3900 and 4000 cm^{-1}, and that the average value of $-\log_{10}R(\tilde{\nu})$ in this region correlates with the EC loading of the filter. When the average baseline from 3900 and 4000 cm^{-1} is calculated, excellent agreement with 5040 EC values is found (r^2 = 0.96), as can be seen in Fig. 9. This spectral region has the additional benefit that no intramolecular vibrational modes of C–H or O–H groups are found in this region, and any overtone or combination bands would be very weak. Therefore, the "baseline" shift can only be caused by the $\pi \rightarrow \pi^*$ electronic transition that would be expected in the spectrum of graphitic materials or PAHs which are believed to constitute the EC component of DPM.

The model used for EC can be written as follows:

$$\mathrm{EC} = \log_{10}(R_{822}) + \langle \log_{10}(R_{4000:3796}) \rangle$$

where R_{822} is the reflectance at 822 cm^{-1} and $R_{4000:3796}$ is the reflectance in the range of 4000 to 3796 cm^{-1}.

3 Summary

It was shown in this study that mid-infrared Fourier transform spectroscopy allows one to correlate both organic and elemental carbons of diesel particulate matter deposited on quartz fiber filters for a wide range of OC/EC ratios, including both lab-generated and in-mine samples. The samples were analyzed using diffuse reflection optics to obtain transflection spectra. The ability to handle a wide range of OC/EC ratios is significant given diesel technology is rapidly evolving and biodiesels are becoming more widely used in the mining environment. NIOSH researchers intend to continue this line of research, with the goals of first demonstrating the efficacy of the method over a wider range of field samples from different mines and working to develop a real-time monitor based on this approach.

This result opens the door to a potential FT-IR-based device which collects an air sample onto a filter medium and analyzes it for EC and OC in near-real time. In essence, the selection of a few bands also sets the stage for a multichannel device based on an infrared source and pyroelectric sensors which target the bands of interest. Future work will explore the use of a partial least squares regression model to improve model accuracy and reduce the number of bands needed for accurate quantification.

Acknowledgements We gratefully acknowledge Nilo Tayag for the analysis of samples. Additionally, we would like to extend our gratitude to Ken Strunk for providing graphics.

Compliance with Ethical Standards

Conflict of Interest The authors declare that they have no conflict of interest.

Disclaimer The findings and conclusions in this report are those of the author(s) and do not necessarily represent the official position of the National Institute for Occupational Safety and Health, Centers for Disease Control and Prevention. Mention of any company or product does not constitute endorsement by NIOSH.

References

1. Cancer IAR (2012) IARC: Diesel engine exhaust carcinogenic, in Press release. World Health Organization
2. Green GM et al (1995) Diesel exhaust: A critical analysis of emissions, exposure, and health effects. HEI (Health Effects Institute)
3. Birch ME (2003) Monitoring of diesel particulate exhaust in the workplace. NIOSH Manual of Analytical Methods (NMAM), p 2154
4. Boffetta P, Jourenkova N, Gustavsson P (1997) Cancer risk from occupational and environmental exposure to polycyclic aromatic hydrocarbons. Cancer Causes & Control 8(3):444–472
5. Pearce F (1997) Devil in the diesel. New Scientist Publ Expediting Inc, Elmont
6. Manabe S et al (1993) Detection of a carcinogen, 2-amino-1-methyl-6-phenylimidazo [4, 5-b] pyridine, in airborne particles and diesel-exhaust particles. Environmental Pollution 80(3):281–286
7. McDonald JD, Campen MJ, Harrod KS, Seagrave JC, Seilkop SK, Mauderly JL (2011) Engine-operating load influences diesel exhaust composition and cardiopulmonary and immune responses. Environ Health Perspect 119(8):1136–1141
8. McDonald JD et al (2011) Engine-operating load influences diesel exhaust composition and cardiopulmonary and immune responses. Environmental Health Perspectives 119(8):1136
9. Noll JD, Janisko S (2013) Evaluation of a Wearable Monitor for Measuring Real-Time Diesel Particulate Matter Concentrations in Several Underground Mines. Journal of Occupational and Environmental Hygiene 10(12):716–722
10. Hansen A, Rosen H, Novakov T (1984) The aethalometer—an instrument for the real-time measurement of optical absorption by aerosol particles. Science of the Total Environment 36:191–196
11. Khan B et al (2012) Differences in the OC/EC ratios that characterize ambient and source aerosols due to thermal-optical analysis. Aerosol Science and Technology 46(2):127–137
12. Harrison RM et al (2013) An evaluation of some issues regarding the use of aethalometers to measure woodsmoke concentrations. Atmospheric Environment 80:540–548
13. Burtscher H (1992) Measurement and characteristics of combustion aerosols with special consideration of photoelectric charging and charging by flame ions. Journal of Aerosol Science 23(6):549–595
14. Weakley AT, Takahama S, Dillner AM (2016) Ambient aerosol composition by infrared spectroscopy and partial least-squares in the chemical speciation network: Organic carbon with functional group identification. Aerosol Science and Technology 50(10): 1096–1114
15. Russell LM, Bahadur R, Ziemann PJJPNAS (2011) Identifying organic aerosol sources by comparing functional group composition in chamber and atmospheric particles. 108(9):3516–3521
16. Weakley AT et al (2018) Ambient aerosol composition by infrared spectroscopy and partial least squares in the chemical speciation network: Multilevel Modeling for Elemental Carbon. 52(6):642–654
17. Dillner A, Takahama SJAMT (2015) Predicting ambient aerosol thermal-optical reflectance (TOR) measurements from infrared spectra: organic carbon. Atmospheric Measurement Techniques 8(3):4013–4023
18. Dillner A, Takahama SJAMT (2015) Predicting ambient aerosol thermal–optical reflectance measurements from infrared spectra: elemental carbon. 8(10):4013–4023
19. Takahama S, Ruggeri G, Dillner AMJAMT (2016) Analysis of functional groups in atmospheric aerosols by infrared spectroscopy: sparse methods for statistical selection of relevant absorption bands. 9(7):3429–3454
20. Burtscher H (2005) Physical characterization of particulate emissions from diesel engines: a review. Journal of Aerosol Science 36(7):896–932
21. Birch M (1999) Elemental carbon (diesel particulate): Method 5040. NIOSH Manual of Analytical Methods (NMAM)
22. Parks DA, Miller AL, Chambers AJ, and Griffiths PR (2018) Investigation of spectroscopic methods for monitoring diesel particulate matter. in SME Annual Meeting Feb. 25–28. 2017. Minneapolis, MN
23. Niyogi S et al (2006) Solution properties of graphite and graphene. Journal of the American Chemical Society 128(24):7720–7721